

DETECTION OF SCALE-SPECIFIC COMMUNITY DYNAMICS USING WAVELETS

TIMOTHY H. KEITT^{1,3} AND JANET FISCHER²

¹Section of Integrative Biology, University of Texas, Austin, Texas 78712 USA

²Department of Biology, Franklin and Marshall College, Lancaster, Pennsylvania 17604 USA

Abstract. The response of ecological communities to anthropogenic disturbance is of both scientific and practical interest. Communities where all species respond to disturbance in a similar fashion (synchrony) will exhibit large fluctuations in total biomass and dramatic changes in ecosystem function. Communities where some species increase in abundance while others decrease after disturbance (compensation) can maintain total biomass and ecosystem function in the face of anthropogenic change. We examined dynamics of the Little Rock Lake (Wisconsin, USA) zooplankton community in the context of an experimental pH manipulation conducted in one basin of the lake. A novel application of wavelets was used to partition patterns of synchrony and compensation by time scale. We find interestingly that some time series show both patterns of synchrony and compensation depending on the scale of analysis. Within the unmanipulated basin, we found subtle patterns of synchrony and compensation within the community, largely at a one-year time scale corresponding to seasonal variation. Within the acidified lake basin, dynamics shifted to longer time scales corresponding to the pattern of pH manipulation. Comparisons between pairs of species in different functional groups showed both strong compensatory and synchronous responses to disturbance. The strongest compensatory signal was observed for two species of *Daphnia* whose life history traits lead to synchrony at annual time scales, but whose differential sensitivity to acidification led to compensation at multiannual time scales. The separation of time scales inherent in the wavelet method greatly facilitated interpretation as patterns resulting from seasonal drivers could be separated from patterns driven by pH manipulation.

Key words: acidification; community variability; compensation; disturbance; Little Rock Lake (Wisconsin, USA); scale; synchrony; wavelets; zooplankton.

INTRODUCTION

The empirical study of coordinated changes in abundance among species has recently emerged as an important topic in ecology because of its potential for generating insights into the structure and organization of ecological communities (Cottingham et al. 2001, Ernest and Brown 2001). This potential is greatly enhanced with the recognition that community variability contains two components: (1) compositional variation in the relative abundance of constituent species and (2) aggregate variation in total individuals or biomass (Micheli et al. 1999). High compositional variation combined with low aggregate variation is called “compensation,” because increases in abundance by one set of species are compensated by decreases among other species. The opposite of compensation, “synchrony” occurs when constituent species increase and decrease simultaneously, leading to high aggregate variability, but low compositional variability.

Community synchrony and compensation play particularly important roles in determining ecosystem re-

sponses to environmental perturbations (Fischer et al. 2001). Compensatory responses serve to stabilize biomass and ecological function in the face of large disturbances: as dominant species within functional groups decline, subdominant species increase in biomass, taking over the ecological role of the former dominant. The result is increased ecological resiliency (Holling 1973). Synchronous dynamics inflate overall variation in biomass leading to reduced resilience. In the most extreme case, if all species exhibit synchronous declines after disturbance, ecosystem function may be severely compromised. However, patterns of synchrony and compensation may vary among functional groups (Fischer et al. 2001), leading to partial failure of ecological function and possibly idiosyncratic long-term community changes as a result of indirect interactions (Ives 1995) or nonlinear thresholds (Carpenter et al. 1992).

Prediction of community responses to disturbance requires detailed mechanistic models of species interactions. These models are difficult to construct and are unlikely to be available across a majority of ecosystems. There is thus a significant need for retrospective methods to assess patterns of synchrony and compensation in community time series. The weakness of retrospective methods is of course that, in the absence

Manuscript received 11 November 2005; revised 4 April 2006; accepted 12 April 2006. Corresponding Editor: D. C. Speirs.

³ E-mail: tkeitt@mail.utexas.edu

of experimental confirmation, true functional compensation leading to resiliency cannot be distinguished from apparent compensation where species show strong negative correlations in abundance because they have opposite responses to some unmeasured time-varying covariate such as temperature. Nonetheless, retrospective methods are important in the detection of community patterns and the generation of hypotheses that may later be tested with true experimental controls. The need for general and flexible diagnostic tools for community time series is further emphasized by the arrival of large synoptic ecosystem data sets (Brown 1995) and proposed efforts, such as the National Ecological Observatory Network (NEON), to generate such datasets on a large scale.

Despite recent advances in retrospective analysis of community time series (Collins et al. 2000, Ives et al. 2003, Sandvik et al. 2004, Vasseur et al. 2005), few studies address the issue of scale in the detection of synchrony and compensation. Explicit consideration of scale is critical to modeling associations between variables measured through time or space as patterns can change both qualitatively and quantitatively with changes in scale of analysis (Keitt and Urban 2005). Here, we apply an alternative method to the detection of synchrony and compensation in community time series that explicitly accounts for hierarchical scale-dependent patterns in data. Our method is based on the wavelet transform (Daubechies 1992), which, like the Fourier transform, is a spectral decomposition that partitions variance according to a precise definition of scale (Mallat 1989). Unlike the Fourier transform and its variants such as the Lomb periodogram (Lomb 1976) that identify dominant frequencies averaged over an entire time series, the wavelet transform permits analysis of nonstationary signals where dominant frequencies change from one moment to the next. Wavelets are therefore particularly suited to signals containing sharp transients, a property typical of environmental time series. The capacity of wavelets to capture transient behavior has led to their widespread application to complex nonlinear phenomena, such as turbulent fluid flow (Muzy et al. 1991), that are unlikely to be efficiently modeled using Fourier methods or linear autoregressive methods. Applications in environmental sciences are beginning to emerge as well (Bradshaw and Spies 1992, Bradshaw and McIntosh 1994, Dale and Mah 1998, Grenfell et al. 2001, Csillag and Kabos 2002, Rosenberg 2004). Here, we use wavelets to quantify scale-dependent patterns in zooplankton community dynamics during the acidification and recovery phases of a whole-lake acidification experiment.

METHODS

Research site and zooplankton species

In 1984, the two basins of Little Rock Lake (LRL), a bilobed seepage lake located in northern Wisconsin, USA, were separated using a vinyl curtain. Following a

year of baseline data collection, sulfuric acid was added to the northern basin (hereafter, acidified basin). The pH of the acidified basin was decreased sequentially to three target levels each maintained for two years: 5.6 (1985–1986), 5.1 (1987–1988), and 4.7 (1989–1990). The recovery phase began in 1991 when all acid additions ceased and the acidified basin was allowed to recover naturally. Throughout the entire study period (1984–2000), the southern basin (hereafter, reference basin) was unmanipulated and served as a reference system for the changes that occurred in the acidified basin. Additional details on the LRL experiment are published elsewhere (Frost et al. 2005).

Samples for enumeration of zooplankton were collected with a 33-L Schindler-Patalas trap (53 m mesh) every two weeks during the ice-free season and approximately monthly during winter. Samples were collected from fixed depths (0, 4, and 8 m in the treatment basin and 0, 4, and 6 m in the reference basin) and preserved with 4% sucrose-buffered formalin. Hypsometrically weighted average abundances were calculated for each basin and zooplankton abundance was converted to biomass using length–mass relationships determined directly for LRL species or from the literature (Frost and Montz 1988). In this study, we focus on six dominant crustacean zooplankton species, including the carnivorous copepods *Diacyclops thomasi* and *Mesocyclops edax*, the herbivorous copepods *Tropocyclops extensus* and *Leptodiaptomus minutus*, and the herbivorous cladocerans *Daphnia dubia* and *Daphnia catawba*. We choose these species pairs because they have been shown previously to exhibit strong either compensatory or synchronous dynamics during the acidification phase of the LRL experiment (Fischer et al. 2001). Specifically, multivariate autoregressive models suggested that the synchronous decline in biomass of carnivorous copepods in the acidified basin was driven by a direct effect of acidification on these two acid-sensitive species. In contrast, herbivorous copepods and cladocerans exhibited compensatory dynamics in the acidified basin. Model results suggested that each of these groups contained acid-sensitive and acid-tolerant species that interacted through competition. Although multivariate autoregressive models are useful for generating and comparing hypotheses about the role of intrinsic and extrinsic factors driving community dynamics (Ives et al. 2003) they do not directly evaluate scale-dependency in the community dynamics. Representative time series from the two LRL basins are shown in Fig. 1.

Time series analysis

Time series were analyzed using the continuous wavelet transform (Daubechies 1992), defined by

$$(T^{\text{wav}}_x)(s, \tau) = \frac{1}{h(s)} \int_{-\infty}^{\infty} \psi\left(\frac{t - \tau}{s}\right) x(t) dt \quad (1)$$

where $x(t)$ is a time series of interest, $\psi([t - \tau]/s)$ represents a wavelet centered at τ and dilated by the

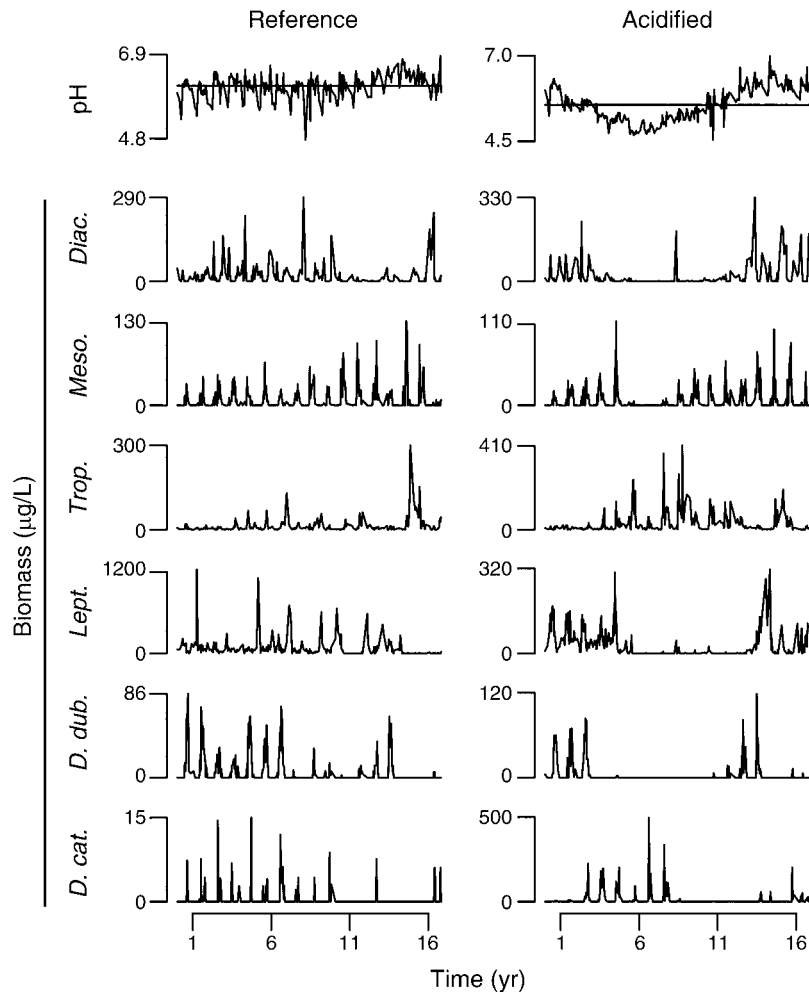


FIG. 1. Time series of Little Rock Lake pH and zooplankton biomass for the reference basin (left column) and the acidified basin (right column). The horizontal line in the pH plots indicates the mean value. Artificial acidification stopped after year 7. Abbreviations: *D. cat.*, *Daphnia catawba*; *D. dub.*, *Daphnia dubia*; *Lept.*, *Leptodiptomus minutus*; *Trop.*, *Tropocyclops extensus*; *Meso.*, *Mesocyclops edax*; *Diac.*, *Diacyclops thomasi*. Data are from the Little Rock Lake Zooplankton Data, North Temperate Lakes Long Term Ecological Research program, funded by NSF (<http://www.limnology.wisc.edu>).

factor s , and $h(s)$ normalizes the wavelet variance for different values of s . A wide variety of wavelets are available for use in the wavelet transform, each quantifying subtly different aspects of the pattern of interest (Mallat 1999).

Because the LRL data were sampled at irregular intervals, we implemented an adaptive “second-generation” wavelet derived conceptually from Sweldens’ (1998) discrete “lifting” transform. Second-generation wavelets have the advantage that they adapt their shape near sampling gaps and boundaries (see Fig. 2), an important consideration for ecological time series which are often short, irregularly sampled, and may contain missing values. Furthermore, adapting the wavelet at the ends of the time series means that artificial boundary adjustments, such as periodic wrapping of the data, are not needed.

In the discrete lifting transform, a time series is split into even ($t = 2, 4, 6, \dots$) and odd ($t = 1, 3, 5, \dots$) numbered samples and then the even numbered samples are predicted by interpolation through the odd numbered samples. The failure of the interpolation to predict the even numbered samples quantifies the variation at frequency π radians ($1/2$ cycle) per sample interval. The predicted values are then “lifted” as input to the next split-predict cycle which quantifies variation at frequency $\pi/2$ radians per sample interval, and so on. The number of lifting stages is limited only by the length of the time series.

Lifting is trivially extended to irregular sampling as the interpolation step does not depend on evenly spaced samples. Many variants on lifting exist, such as use of spline interpolation methods (Sweldens 1998). Jansen et al. (2001), for example, use linear regression to predict

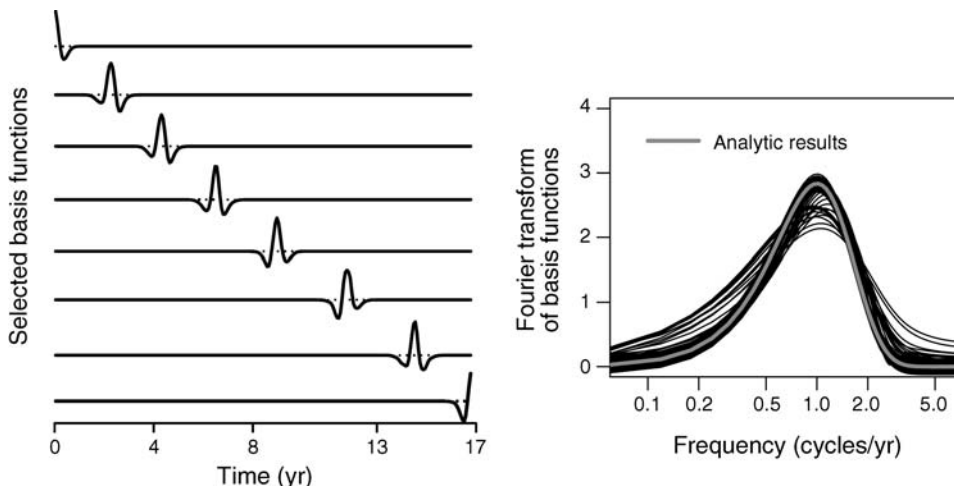


FIG. 2. Illustration of the adaptive “Difference-of-Gaussians” wavelet. The left-hand panel shows selected basis functions (wavelets) used in the analysis described in this paper. The slight asymmetries in the wavelets resulted from irregular sampling. The right-hand panel shows the Fourier transform of 256 of these basis functions along with the analytic result (thick gray line). A small random vertical offset was added to each of the numerical results (black lines, right-hand panel) so that they would not be completely obscured by the analytic results.

each point from a set of nearest neighbors. Previous applications of lifting have focused on the discrete transform where the scale of analysis progresses as a geometric series, typically doubling at each level of analysis. For our purposes, the continuous wavelet transform is far more informative as the scale of analysis can be continuously adjusted.

To construct a continuous second-generation wavelet transform, we extended the idea of regression on nearest neighbors to the more general concept of local regression (Loader 1999). Local regression methods estimate the mean of input data conditionally at each point of interest using locally defined regression weights. The weights generally decay as a smooth function of distance. A special case of local regression is the Nadaraya-Watson estimator,

$$\eta_{s,\tau}(t) = \frac{k\left(\frac{t-\tau}{s}\right)}{\sum_{u \in \Omega} k\left(\frac{u-\tau}{s}\right)} \tag{2}$$

which is equivalent to a local regression model with only a single intercept term (Hastie and Loader 1993). Here, $\Omega = \{t_1, t_2, t_3, \dots, t_n\}$ are the sample locations, τ is the point of interest and s along with the kernel function k determines the rate at which regression weights decay with distance. The Gaussian kernel $k(t) = e^{-t^2/2}$ was used in all subsequent analyses.

Local regression can be thought of as a signal filter that separates high frequency variation, in the form of residual errors, from low frequency variation contained in the local averages. How much of the high frequency variation is removed depends on the bandwidth parameter s . Isolation of intermediate frequencies, the goal of scale-specific analysis, can be accomplished by subtraction of local regression estimators as follows:

$$\psi_{s,\tau}(t) = \eta_{s,\tau}(t) - \eta_{s',\tau}(t) \tag{3}$$

with bandwidths s and s' , resulting in a second-generation variant of the “Difference-of-Gaussians” (DoG) wavelet (Muraki 1995). The ratio $\beta = s'/s$ determines the shape of the DoG wavelet and its band-pass characteristics. For convenience, we chose $\beta = 1.87$ such that for any scaling $t \rightarrow t/s$, the dominant scale of analysis was simply s time units. To arrive at the chosen value, we note that Fourier transform of the DoG wavelet is given by

$$(T^{\text{Fourier}} \psi_{s,\tau})(\omega) = e^{-s^2\omega^2/2} - e^{-\beta^2 s^2\omega^2/2} \tag{4}$$

which attains its maximum at

$$\omega = \frac{2\sqrt{\ln\beta}}{s\sqrt{\beta^2 - 1}} \tag{5}$$

Substituting $\beta = 1.87$ into Eq. 5 yields a maximum transfer of variance at frequency $\omega = 1/s$, or equivalently, one cycle per s time units. Examples of the adaptive DoG wavelet and their Fourier transforms are shown in Fig. 2.

Evaluated over a set of discrete samples Ω , the adaptive wavelet transform is given by

$$(T^{\text{wav}} x)(s, \tau) = \frac{1}{h_\tau(s)} \sum_{t \in \Omega} \psi_{s,\tau}(t)x(t) \tag{6}$$

where

$$h_\tau(s) = \sqrt{\sum_{t \in \Omega} [\psi_{s,\tau}(t)]^2} \tag{7}$$

ensures that wavelet variances are comparable across all locations and scales. The major difference between Eqs. 1 and 6 is that the latter depends explicitly on the sample

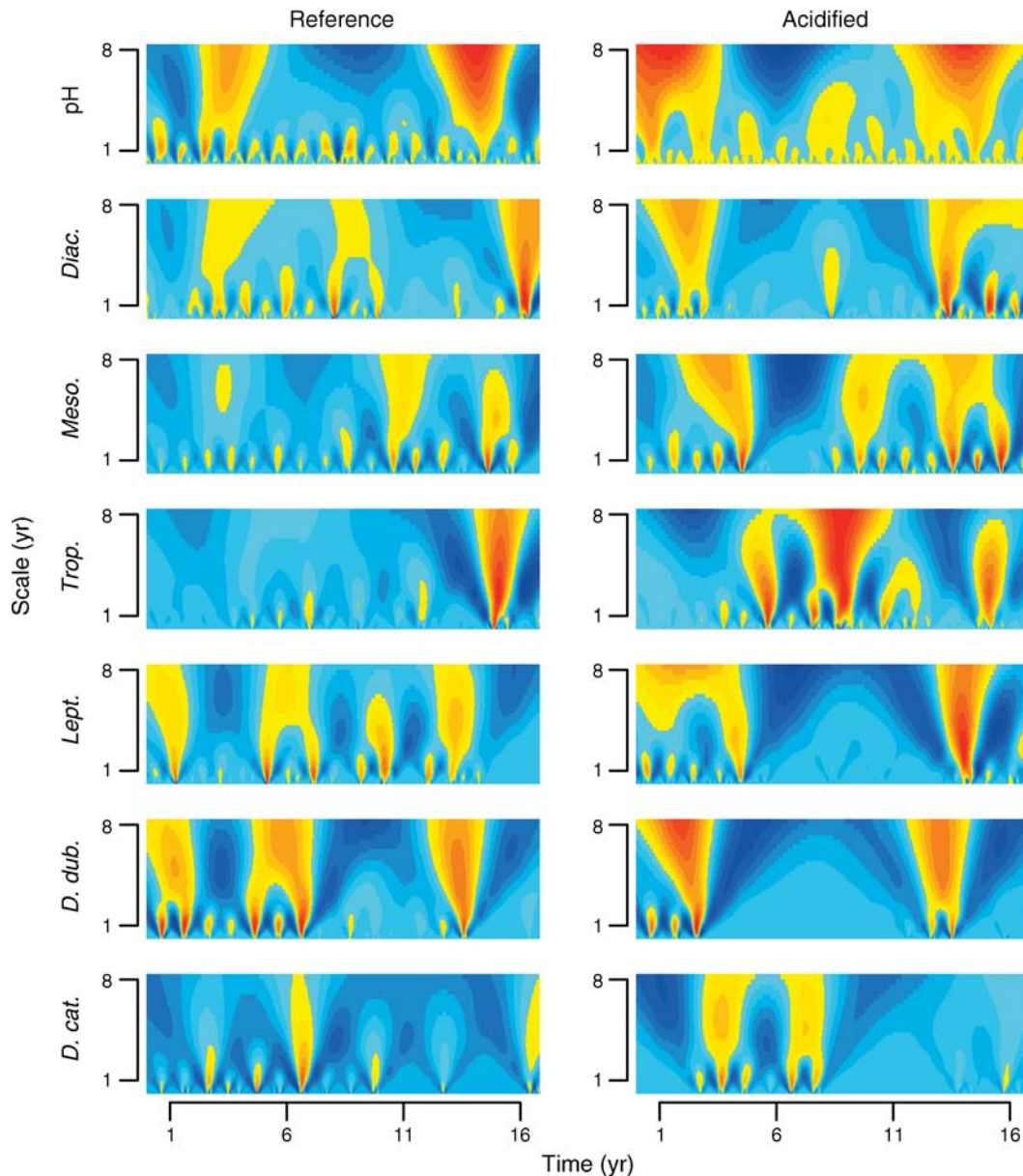


FIG. 3. Scale–location plots for pH and six zooplankton species in the reference basin (left column) and acidified treatment basin (right column). The time scale increases vertically. Colors indicate magnitudes of the wavelet coefficients at different scales: blue indicates strong negative values, and red indicates strong positive values; cyan and yellow cells correspond to smaller-magnitude negative and positive values, respectively. Abbreviations are as in Fig. 1.

locations Ω . (Despite the sum in Eq. 6, the adaptive transform remains continuous as s and τ can be varied continuously.)

Wavelet statistics

Scale–location plots were used as a graphic depiction of the wavelet transform. The coefficients $(T^{\text{wav},x})(s, \tau)$ were plotted as an image with scale s increasing vertically and location τ aligned to the horizontal axis. A color scale was used to indicate the relative magnitudes of the coefficients (see Fig. 3).

Wavelet covariances were used to quantify scale-dependent relationships between time series. Wavelet covariance for the set of discrete sample events Ω was defined as

$$\Theta_s(u, v) = \sum_{\tau \in \Omega} [(T^{\text{wav}}u)(s, \tau) \times (T^{\text{wav}}v)(s, \tau)] \quad (8)$$

where s is the scale of analysis and u and v are time series of interest. The special case $u = v$ computes the wavelet variance (Percival 1995), which quantifies the intensity of pattern present at scale s (see Fig. 4).

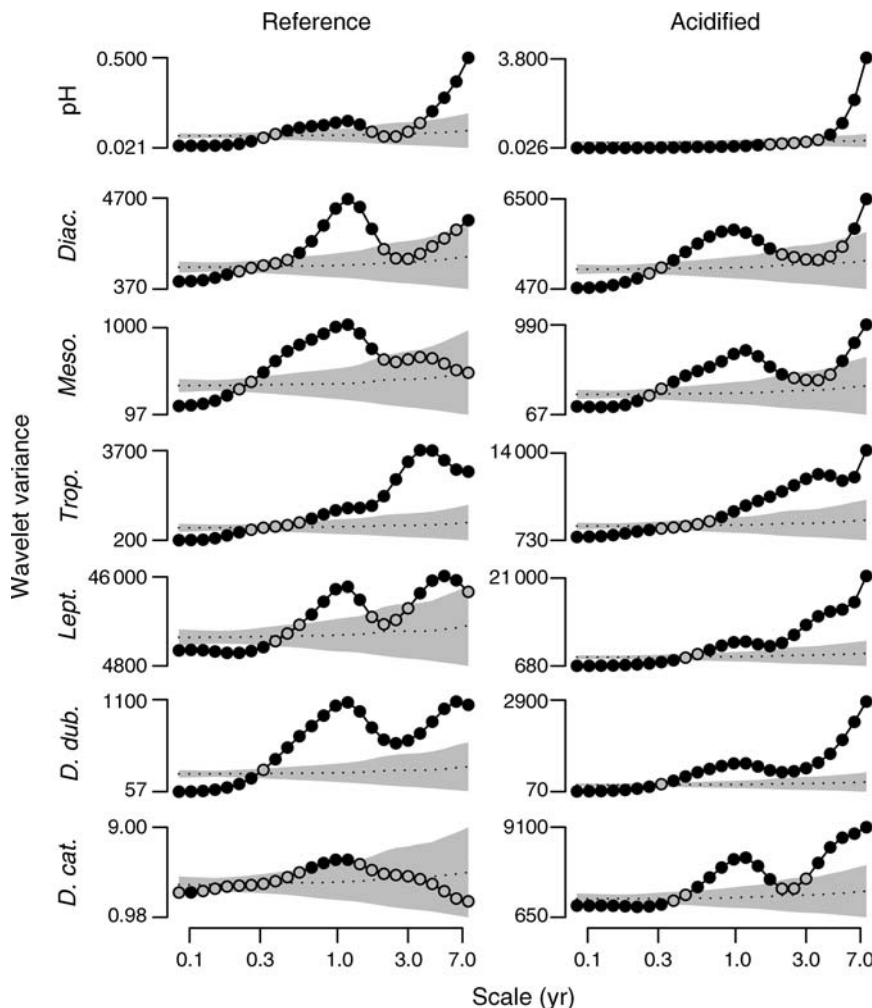


FIG. 4. Wavelet variance by scale for the reference basin (left column) and acidified treatment basin (right column). Gray regions bound 95% confidence limits obtained from 1×10^4 random permutations of the original time series. Solid black circles indicate values falling outside the bootstrap confidence intervals. Note that the x -axis is log-transformed to show more detail at shorter time scales. Abbreviations are as in Fig. 1.

Statistical significance of observed covariances was assessed by repeated permutation of the original time series. For each of 1×10^4 permutations, wavelet covariances were recorded. Confidence intervals were then generated encompassing 95% of the simulated covariances. Observed $\Theta_s(u, v)$ values falling outside of the resulting confidence intervals were considered to deviate significantly from the null hypothesis of no pattern.

RESULTS

Scale–location plots and wavelet variances for individual species

A variety of patterns were present in scale–location plots of the wavelet transformed time series (Fig. 3). Annual cycles appeared as alternating blue–cyan and yellow–red regions near the bottom of the scale–location

plots. Multi-year trends were identified by alternating blue–cyan and yellow–red patterns near the top of the scale–location plots. Although all of the species exhibited some degree of annual cycling, *Mesocyclops* showed the most consistent annual pattern. Other species showed episodes of annual cycling punctuated by periods of relative quiescence (generally corresponding to periods of low abundance).

Wavelet variance results showed significant annual periodicity for all species (Fig. 4). In the reference basin, the presence of multi-year trends varied among species. For example, *Mesocyclops* and *D. catawba* did not show any significant variation beyond the annual time scale in the reference basin, unlike all remaining species that did show this pattern. We observed a marked increase in multi-year variances for all species in the acidified basin, indicating a strong response to pH manipulation. All of the time series showed significantly less variability

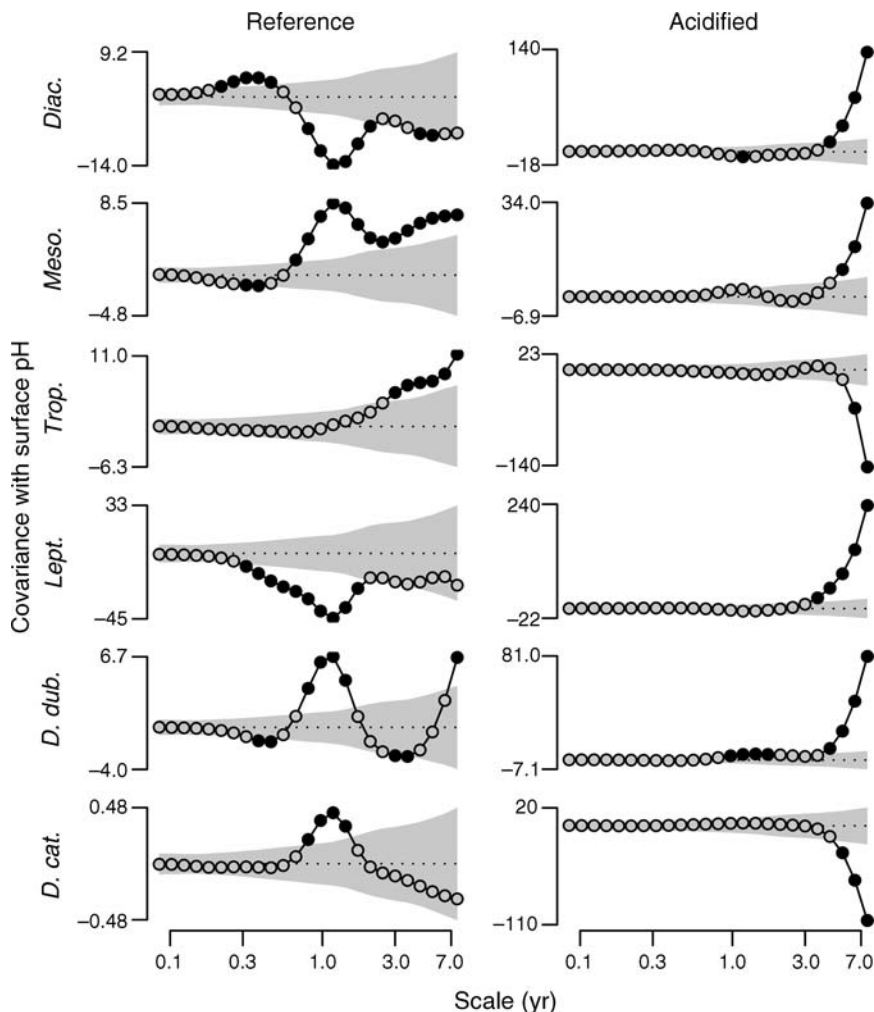


FIG. 5. Covariance between zooplankton species and pH as a function of time scale for the reference basin (left column) and acidified treatment basin (right column). Gray regions bound 95% confidence limits obtained from 1×10^4 random permutations of the original time series. Solid black circles indicate values falling outside the bootstrap confidence intervals. Note that the x-axis is log-transformed to show more detail at shorter time scales. Abbreviations are as in Fig. 1.

relative to the resampled time series at sub-annual scales, indicating short-range dependencies between successive values (Fig. 4). Notice that in no case did the randomized time series (which shared the same sampling time points as the real time series) show a peak in variance at the annual time scale, indicating that the slight seasonal variation in sampling frequency could not have been responsible for the annual scale peaks observed in the real data.

pH

Surface pH showed a distinct pattern of annual variation in both reference and acidified basins, as well as strong variation over multiple years. The intensity of the multi-year variation was greater in the acidified basin as a result of the experimental acidification (Fig. 4). Interestingly, annual variability was somewhat reduced in the treatment basin relative to the reference

basin, particularly in earlier phases when pH was being actively manipulated. Also of interest was the presence of a multi-year trend in pH in the reference basin, indicating a natural background trend in pH, albeit not as large in magnitude as in the acidified basin.

Carnivorous copepods

In the reference basin, the carnivorous copepods *Diaacyclops* and *Mesocyclops* exhibited contrasting patterns of scale-dependent covariance with pH. For *Diaacyclops*, covariance with pH shifted from positive to negative with increasing time scale, whereas *Mesocyclops* exhibited the opposite pattern (Fig. 5). In the acidified basin, where pH changes were more dramatic due to the manipulation, both *Diaacyclops* and *Mesocyclops* showed strong positive covariation with pH at the longest time scales, indicating a simultaneous decrease in pH and abundance (Fig. 5). Covariance

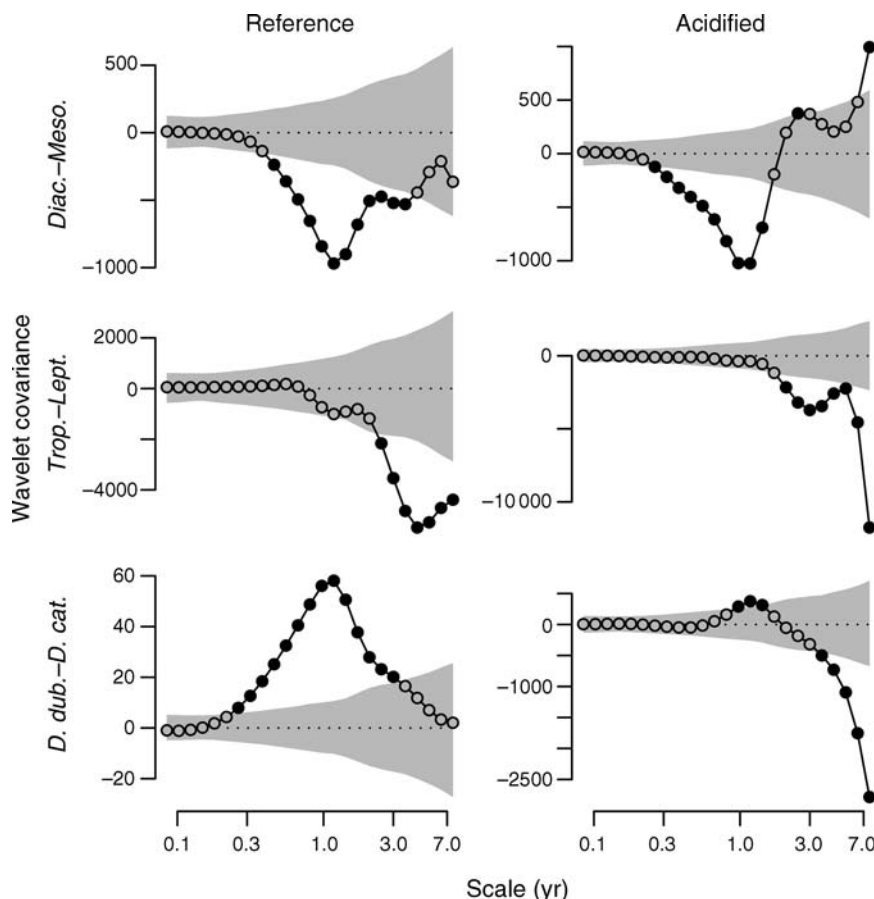


FIG. 6. Covariance between zooplankton species pairs as a function of time scale for the reference basin (left column) and acidified treatment basin (right column). Gray regions bound 95% confidence limits obtained from 1×10^4 random permutations of the original time series. Solid black circles indicate values falling outside the bootstrap confidence intervals. Note that the x-axis is log-transformed to show more detail at shorter time scales. Abbreviations are as in Fig. 1.

between *Diaacyclops* and *Mesocyclops* was strongly negative in the reference and acidified basin at annual time scales (Fig. 6). At the longest time scales analyzed, strong positive covariance between *Diaacyclops* and *Mesocyclops* emerged in the acidified basin, probably due to parallel declines in *Diaacyclops* and *Mesocyclops* abundance during the acidification phase of the experiment.

Herbivorous copepods

In the reference basin, the herbivorous copepod *Tropocyclops* exhibited positive covariance with pH at the longest time scales, whereas *Leptodiaptomus* showed negative covariance with pH at the annual time scale (Fig. 5). In the acidified basin, the two herbivorous copepods exhibited contrasting patterns of covariance with pH at the longest time scales. Specifically, covariance with pH was strongly negative for *Tropocyclops* and positive for *Leptodiaptomus*. In both reference and acidified basins, covariance between *Tropocyclops* and *Leptodiaptomus* was negative at 3–4 yr time scale (Fig. 6). In the acidified basin, this 3–4 yr signal in

covariance between the two species was accompanied by a strong spike in negative covariance at the longest time scales (Fig. 6). Interestingly, maximum absolute covariance was approximately threefold larger in the acidified basin than in the reference basin.

Herbivorous cladocerans

In the reference basin, both *D. dubia* and *D. catawba* exhibited positive covariance with pH at annual time scales (Fig. 5). Similar to other species, patterns of covariance with pH in the acidified basin were more dramatic at the longest time scales, where *D. dubia* showed strong positive covariance with pH and *D. catawba* exhibited strong negative covariance with pH. These patterns are clearly visible in the original time series (Fig. 1). In both acidified and reference basins, *D. dubia* and *D. catawba* showed highly synchronous annual cycles. We observed a 10-fold increase in the magnitude of the positive annual covariance between *D. dubia* and *D. catawba* in the acidified basin, as well as the addition of strong compensation at the longest time scales.

DISCUSSION

The LRL zooplankton time series exhibited two hallmarks of complexity: variability across a wide range of time scales and intermittent dynamical shifts (Stanley et al. 2000). The pattern of intermittency was clearly captured in the wavelet scale–location plots (Fig. 3), where species dynamics shifted between regular annual cycles and quiescent periods with little or no variation at the annual scale. Sharp spikes in abundance were also observed, such as can be seen near the end of the *Diacyclops* and *Tropocyclops* time series. The local nature of the wavelet transform means that these sorts of events can be efficiently characterized. Sharp transients can introduce bias when applying non-local methods, such as the Fourier transform, because such events are not easily represented by regularly oscillating functions. This is not to say that non-local methods should not be applied. In the case of regular sinusoidal patterns, Fourier methods can more precisely isolate dominant frequencies compared to the localized wavelet transform.

Within the context of complex dynamics, clear patterns of synchrony and compensation did emerge in patterns of wavelet covariance for pairs of species. In some cases, species pairs exhibited both synchrony and compensation within the same basin, depending on the scale of analysis. At the annual time scale, variation in biomass was strongly entrained to seasonal climate variation, and this abiotic signal could influence aspects of species interactions. The herbivorous cladocerans, *D. dubia* and *D. catawba*, for example, exhibited strongly synchronous annual variation. These species are absent from the water column during the winter, hatch from dormant eggs shortly after ice-off each spring, and are usually present in the water column until temperatures begin to cool in the fall (De Stasio 1990). The herbivorous copepods, however, exhibited compensatory annual variation. In Little Rock Lake, *Mesocyclops* dominates during the summer months, but *Diacyclops* is abundant in the fall, winter, and spring. This species shift may be driven by competition for a shared food resource or opposite responses to seasonal variation in other environmental factors (i.e., apparent compensation).

At longer time scales, the effects of the pH manipulation were apparent in patterns of wavelet covariance for species pairs in the acidified basin. Carnivorous copepods declined dramatically during the final stage of the acidification, and this response was evident in the positive covariance with pH for both of these species and the strong positive covariance of the species pair at the longest time scale. Autoregressive models fit to these data support the conclusion that the observed positive covariance was a direct effect of pH stress on these two acid-sensitive species (Fischer et al. 2001). In contrast, herbivorous copepods and herbivorous cladocerans exhibited compensatory dynamics in response to acidification, as indicated by the strong wavelet covariance for these species pairs at the longest time scales. As the

species-specific patterns of covariance with pH suggest, each pair contained one acid-sensitive and one acid-tolerant species. Short-term bioassays indicate that *Leptodiptomus* and *D. dubia* are acid sensitive, whereas *Tropocyclops* and *D. catawba* are more tolerant (Fischer 1997). This composition, along with competitive interactions between species, can generate a resilient response to environmental fluctuations (Ives 1995, Fischer et al. 2001).

The wavelet transform is a highly flexible tool for extracting localized, scale-specific information from data. Although not explored here, there exists a wide array of wavelets, each emphasizing subtly different aspects of pattern. The major consideration in choosing a wavelet is the trade-off between strong localization, which is good for analyzing sharp transients, vs. weak localization, but more precise isolation of dominant frequencies. Other properties of wavelets may also be selected, such as symmetry and overall smoothness. Many software packages provide routines to optimally select wavelets for a given data set, and this would be an interesting avenue for future studies. It would also be interesting to explore fitting parametric regression or process-driven models to wavelet-transformed community time series data (e.g., see Keitt and Urban [2005]).

Overall, our results highlight the utility of wavelet analysis for quantifying scale-dependent shifts in community dynamics. Analyzing data in a scale-dependent manner is particularly helpful in situations where physical forcing of community dynamics occurs at widely different time scales, as was the case in our analysis of the LRL zooplankton community. Application of the wavelet transform allowed us to clearly identify a shift toward multi-annual variation in the acidified basin paralleling the time scale at which pH was manipulated. The long-term variation in the acidified basin contrasted sharply with the more subtle annual-scale variation observed in the reference basin. The ability of the wavelet approach to detect and contrast patterns occurring at different time scales has strong relevance to the general problem of disentangling external abiotic drivers of community dynamics from internal dynamics resulting from processes of population growth and interactions. In the context of global change, scale-dependent analysis may prove useful in detecting changes in community dynamics resulting from anthropogenic factors, which may have complex tempos and scales far different from those naturally present in a given community.

ACKNOWLEDGMENTS

We thank M. Leibold for constructive comments on an early version of the manuscript. T. Keitt acknowledges the generous support of the David and Lucile Packard Foundation. The Little Rock Experimental Acidification Project has been supported by funding from the National Science Foundation, the U.S. Environmental Protection Agency, the U.S. Geological Survey, and the state of Wisconsin. It has also received logistic assistance from the North Temperate Lakes Long Term Ecological Research Program.

LITERATURE CITED

- Bradshaw, G. A., and B. A. McIntosh. 1994. Detecting climate-induced patterns using wavelet analysis. *Environmental Pollution* **83**:135–142.
- Bradshaw, G. A., and T. A. Spies. 1992. Characterizing canopy gap structure in forests using wavelet analysis. *Journal of Ecology* **80**:205–215.
- Brown, J. H. 1995. *Macroecology*. The University of Chicago Press, Chicago, Illinois, USA.
- Carpenter, S. R., C. E. Kraft, R. Wright, X. He, P. A. Spranno, and J. R. Hodgson. 1992. Resilience and resistance of a lake phosphorus cycle before and after food web manipulation. *American Naturalist* **140**:781–798.
- Collins, S. L., F. Micheli, and L. Hartt. 2000. A method to determine rates and patterns of variability in ecological communities. *Oikos* **91**:285–293.
- Cottingham, K. L., B. L. Brown, and J. T. Lennon. 2001. Biodiversity may regulate the temporal variability of ecological system. *Ecology Letters* **4**:72–85.
- Csillag, F., and S. Kabos. 2002. Wavelets, boundaries, and the spatial analysis of landscape pattern. *Ecoscience* **9**:177–190.
- Dale, M. R. T., and M. Mah. 1998. The use of wavelets for spatial pattern analysis in ecology. *Journal of Vegetation Science* **9**:805–814.
- Daubechies, I. 1992. Ten lectures on wavelets. CBMS-NSF Regional Conference Series in Applied Mathematics, Society for Industrial and Applied Mathematics, Philadelphia, Pennsylvania, USA.
- De Stasio, B. T., Jr. 1990. The role of dormancy and emergence in the dynamics of a freshwater zooplankton community. *Limnology and Oceanography* **35**:1079–1090.
- Ernest, S. K. M., and J. H. Brown. 2001. Homeostasis and compensation: the role of species and resources in ecosystem stability. *Ecology* **82**:2118–2132.
- Fischer, J. M. 1997. Zooplankton community responses to acidification: the role of rapid evolution and compensatory dynamics. Dissertation, University of Wisconsin, Madison, Madison, Wisconsin, USA.
- Fischer, J. M., T. M. Frost, and A. R. Ives. 2001. Compensatory dynamics in zooplankton community responses to acidification: measurement and mechanisms. *Ecological Applications* **11**:1060–1072.
- Frost, T. M., J. M. Fischer, P. L. Brezonik, M. J. Gonzalez, T. K. Kratz, C. J. Watras, and K. E. Webster. 2005. The experimental acidification of Little Rock Lake. Pages 168–186 in J. J. Magnuson, T. K. Kratz, and B. J. Benson, editors. Long-term dynamics of lakes in the landscape. Oxford University Press, New York, New York, USA.
- Frost, T. M., and P. M. Montz. 1988. Early zooplankton response to experimental acidification of Little Rock Lake, Wisconsin, USA. *Internationale Vereinigung für Theoretische und Angewandte Limnologie* **23**:2279–2285.
- Grenfell, B. T., O. N. Bjornstad, and J. Kappey. 2001. Travelling waves and spatial hierarchies in measles epidemics. *Nature* **414**:716–723.
- Hastie, T., and C. Loader. 1993. Local regression: automatic kernel carpentry. *Statistical Science* **8**:120–129.
- Holling, C. S. 1973. Resilience and stability in ecological systems. *Annual Reviews in Ecological Systems* **4**:1–23.
- Ives, A. R. 1995. Predicting the response of populations to environmental change. *Ecology* **76**:926–941.
- Ives, A. R., B. Dennis, K. L. Cottingham, and S. R. Carpenter. 2003. Estimating community stability and ecological interactions from time-series data. *Ecological Monographs* **73**:301–330.
- Jansen, M., G. P. Nason, and B. W. Silverman. 2001. Scattered data smoothing by empirical Bayesian shrinkage of second generation wavelet coefficients. Pages 87–97 in M. Unser and A. Aldroubi, editors. Wavelet applications in signal and image processing. Proceedings of SPIE, volume 4478. SPIE—The International Society for Optical Engineering, Bellingham, Washington, USA.
- Keitt, T. H., and D. L. Urban. 2005. Scale-specific inference using wavelets. *Ecology* **86**:2497–2504.
- Loader, C. 1999. *Local regression and likelihood*. Statistics and computing. Springer, New York, New York, USA.
- Lomb, N. R. 1976. Least-squares frequency analysis of unequally spaced data. *Astrophysics and Space Science (Historical Archive)* **39**:447–462.
- Mallat, S. G. 1989. A theory for multiresolution signal decomposition: the wavelet representation. *IEEE Transactions on Pattern Analysis and Machine Intelligence* **11**:674–693.
- Mallat, S. 1999. *A wavelet tour of signal processing*. Second edition. Academic Press, New York, New York, USA.
- Micheli, F., K. L. Cottingham, J. Bascompte, O. N. Bjornstad, G. L. Eckert, J. M. Fischer, T. H. Keitt, B. E. Kendall, J. L. Klug, and J. A. Rusak. 1999. The dual nature of community variability. *Oikos* **85**:161–169.
- Muraki, S. 1995. Multiscale volume representation by a DOG wavelet. *IEEE Transactions on Visualization and Computer Graphics* **1**:109–116.
- Muzy, J. F., E. Bacry, and A. Arneodo. 1991. Wavelets and multifractal formalism for singular signals: Application to turbulence data. *Physical Review Letters* **67**:3515–3518.
- Percival, D. B. 1995. On estimation of the wavelet variance. *Biometrika* **82**:771–787.
- Rosenberg, M. S. 2004. Wavelet analysis for detecting anisotropy in point patterns. *Journal of Vegetation Science* **15**:277–284.
- Sandvik, G., C. M. Jessup, K. L. Seip, and B. J. M. Bohannan. 2004. Using the angle frequency method to detect signals of competition and predation in experimental time series. *Ecology Letters* **7**:640–652.
- Stanley, H. E., L. A. N. Amaral, P. Gopikrishnan, P. C. Ivanov, T. H. Keitt, and V. Plerou. 2000. Scale invariance and universality: organizing principles in complex systems. *Physica A: Statistical Mechanics and its Applications* **281**:60–68.
- Sweldens, W. 1998. The lifting scheme: a construction of second generation wavelets. *SIAM Journal on Mathematical Analysis* **29**:511–546.
- Vasseur, D. A., U. Gaedke, and K. S. McCann. 2005. A seasonal alteration of coherent and compensatory dynamics occurs in phytoplankton. *Oikos* **110**:507–514.